

TRIBOLOGICAL BEHAVIOUR OF IRON-ALUMINIUM ALLOY

A THESIS SUBMITTED IN PARTIAL FULFILMENT OF
THE REQUIREMENTS FOR THE DEGREE OF

Master of Technology
In
Mechanical Engineering
(Steel technology)

BY

PANKAJ KUMAR
(Roll No- 213MM2484)



Department of Metallurgical and Materials Engineering
National Institute of Technology
Rourkela-769008, 2015

TRIBOLOGICAL BEHAVIOUR OF IRON-ALUMINIUM ALLOY

A THESIS SUBMITTED IN PARTIAL FULFILMENT OF
THE REQUIREMENTS FOR THE DEGREE OF

Master of Technology
In
Mechanical Engineering
(Steel technology)

BY

PANKAJ KUMAR
(Roll No- 213MM2484)

Under Supervision of
Prof. S.C. MISHRA



Department of Metallurgical and Materials Engineering
National Institute of Technology
Rourkela-769008, 2015



National Institute of Technology

Rourkela

CERTIFICATE

This is to certify that thesis entitled, “***TRIBOLOGICAL BEHAVIOUR OF IRON-ALUMINUM ALLOY***” submitted by **Mr. Pankaj Kumar** bearing (**Roll No. 213MM2484**) partial fulfilment of the requirements for the award of **Master of Technology** Degree in Mechanical Engineering (Steel Technology) at National Institute of Technology, Rourkela is an authentic work carried out by him under my supervision and guidance.

To the best of our knowledge, the matter embodied in this thesis has not been submitted to any other university/ institute for award of any Degree or Diploma.

Date:

Prof. S.C. Mishra

Department of Metallurgical and Materials

Engineering

National Institute of Technology

Rourkela-769008

ACKNOWLEDGEMENT

I would like to express my deep sense of gratitude and respect to my supervisor cum Head of Department Metallurgical and Materials Engineering **Prof. S.C. Mishra** for his invaluable guidance, motivation, constant inspiration and above all for his ever co-operating attitude that enabled me in bringing up this thesis in the present form.

I consider myself extremely lucky to be able to work under the guidance of such a dynamic personality and for providing me necessary facilities in the department.

I would like to thank **Ranjan Behera** (Ph.D. Scholar, Department of Metallurgical and Materials Engineering), and my all friends with whose additional help in this study has been a succulent one.

My very special thanks go to all my family members. Their love, affection and patience made this work possible and the blessings and encouragement of my beloved parents greatly helped me in carrying out this research work.

Date:

PANKAJ KUMAR

213MM2484

ABSTRACT

Iron-Aluminium based alloys have a significant prospective for operational applications at elevated temperature as they retain an outstanding elevated temperature corrosion resistance and they possess a lower density compared to other Iron- base materials such as cast iron and stainless steels. Material cost of Iron-Aluminium based alloys is comparably low because their manufacturing and handling process are widely available. Fe-Al alloy is gaining its attractiveness in many business applications due to its wear properties and erosion properties, which is because of the presence of Al.

The current study is focused on investigating the mechanical properties and tribological behaviour of Fe-Al alloy (Fe wt%94.18 and Al wt% 5.82) to various heat treatment processes. In this investigation we deal with the analysis of microstructure by means of microscope, crystalline phases and its structural properties by means of XRD analysis. Specimens are heat treated at different temperature (400⁰C, 600⁰C, 800⁰C and 1200⁰C) and then quenched. The soaking time being 2 hours and quenching media is simply water. After heat treatment, we have to investigate the comparison between mechanical properties and behaviour of the material by means of metallography, XRD analysis and Vickers hardness test. After Vickers hardness test, erosion properties are measured by means of Air jet

erosion test rig machine. It is found that water quenched from 1200⁰C heated sample shows slightly increase in hardness, which is mainly due to new phase Al₅W reveals in XRD pattern with highest intensity. XRD analysis shows that all samples of Fe-Al alloy are of BCC structure. Erosion wear test was executed on Fe-Al alloy by air jet erosion test rig. The volume of removed material gives the measurement of erosion wear at impact angles 30⁰, 60⁰ and 90⁰. It is found that all heat treated samples (except quenched from 1200⁰C sample) having maximum disinterested material volume at 60⁰ impact angles, which shows that all samples are semi ductile. But in case of quenched from 1200⁰C sample having maximum removed material volume is at 90⁰ impact angle, shows brittle in nature. So it was shown that Fe-Al alloy with proper heat treatment has outstanding erosion resistance and it is estimated to find extensive applications as a wear resistant material.

KEY WORDS: Iron-Aluminium alloys, mechanical properties, microstructure analysis, XRD analysis, Erosion wear test

CONTENTS

	PAGE NO.
CERTIFICATE	i
ACKNOWLEDGEMENT	ii
ABSTRACT	iii
CONTENTS	v
LIST OF FIGURES	viii
LIST OF TABLES	x
CHAPTER 1 INTRODUCTION	1
1.1 Introduction	2
1.1.1 Tribology science	2
1.1.2 Wear	3
1.2 History of Al	3
1.3 Importance of aluminium in iron and steel	4
1.4 Mechanical property of iron-aluminium alloy	5
1.5 Miscellaneous uses of aluminium in iron and steel	8
1.5.1 Heat resisting alloys	8
1.5.2 Nitriding steels	9
1.5.3 Aluminizing	9

1.5.4 Tool steel	9
CHAPTER 2 LITERATURE SURVEY	11
2.1 Introduction	12
2.2 Phase diagram of Fe-Al alloy	12
2.3 Constitution of iron rich Fe-Al-C alloys	14
2.4 Factors affecting the ductility of Fe-Al alloy	16
2.4.1 Influence of annealing treatments in ductility	16
2.4.2 Influence of grain size on ductility	18
2.4.3 Influence of substitutional alloying on ductility	19
2.4.4 Influence of molybdenum on ductility	21
2.4.5 Influence of carbon on ductility	21
2.4.6 Effect of temperature on yield strength	22
2.5. Melting and working of Iron-Aluminium alloys	23
CHAPTER 3 EXPERIMENTAL PROCEDURE	25
3.1 Introduction	25
3.2 Material compositions	25
3.3 Metallographic	25
3.4 X-Ray diffraction studies	26
3.5 Heat treatment	27

3.6 Vickers hardness test	27
3.7 Air Jet Erosion Test Rig machine	28
CHAPTER 4 RESULTS AND DISCUSSION	32
4.1 Microstructure analysis	33
4.1.1 Microstructure before heat treatment	33
4.1.2 Microstructure analysis after heat treatment	34
4.2 SEM-EDS Analysis	35
4.3 XRD Phase composition analysis	36
4.3.1 XRD before heat treatment	36
4.3.2 XRD after heat treatment	37
4.4 Vickers hardness test	40
4.5 Air Jet Erosion test	41
CHAPTER 5 CONCLUSION	44
5.1 Conclusions	45
REFERENCES	48

INDEX OF FIGURES

Fig. No	DESCRIPTION	Page No.
1.1	Mechanical properties of Iron –Aluminium alloy (T.D Yensen& W.A Gatward)	6
2.1	Thermal equilibrium diagram of the iron-aluminium system, showing phase fields of ordered and disordered alloys (A.Taylor & R.M.Jones)	13
2.2	Fe-rich part of the, isothermal section of the ternary Fe–Al–C system at 800 ⁰ C	15
2.3	Influence of heat treatments on yield stress and tensile ductility of Fe±40Al containing 0.6% carbon	18
2.4	Changes of yield stress and tensile ductility with additions various alloying elements (Mo, Nb, W)	20
2.5	Yield strength with respect to testing temperature for iron rich Iron-Aluminium alloy	22
3.1	XRD machine	26
3.2	Arrangement of erosion test rig. (1) Sand hopper, (2) Conveyor belt system for abrasive particles, (3) Pressure	28

	transducer, (4) Particle air mixing chamber, (5) Nozzle, (6) X– Y and h axis assembly, (7) Sample holder.	
4.1	Microstructure of specimen before heat treatment.	32
4.2	Microstructure of heat treated sample at temperature fig (a) 400 ⁰ C (b) 600 ⁰ C (c) 800 ⁰ C and (d) 1200 ⁰ C.	33
4.3	EDS analysis of Fe-Al alloy.	34
4.4	XRD pattern before heat treatment	36
4.5	XRD pattern of heat treated specimen at temperature, fig (a) 400°C (b) 600°C (c) 800°C (d) 1200°C	38
4.6	Hardness of specimens at different heat treatment temperature.	39
4.7	Mean weight loss of heat treated sample at different temperature with respect to impact angles.	41

INDEX OF TABLES

TABLE NO.	DESCRIPTION	PAGE NO.
Table-3.1	Chemical composition of samples.	25
Table 3.2	Technical Specification for Air Jet Erosion Test rig (ASTM G76 standard).	30
Table4. 1	Chemical composition of the structure.	34

Chapter

1

INTRODUCTION

1.1 Introduction

1.1.1 Tribology science

1.1.2 Wear

1.2 History of Al

1.3 Importance of aluminium in iron and steel

1.4 Mechanical property of iron-aluminium alloy

1.5 Miscellaneous uses of aluminium in iron and steel

1.5.1 Heat resisting alloys

1.5.2 Nitriding steels

1.5.3 Aluminizing

1.5.4 Tool steel

1.1 Introduction

Iron–Aluminium based alloys have a significant prospective for operational applications at elevated temperatures as they have an extraordinary elevated temperature corrosion resistance [1] and they possess lower density examine in contrast to other iron- base materials, for example, stainless steels an cast iron . Fe–Al- based alloys additionally offer equivalently low material expenses because of their manufacturing and handling are broadly accessible .In perspective of their melting temperatures, which might be generally in range between 1200° to 1400°C, Iron–Aluminium based alloys may be utilized for operational applications up to administration temperatures of 1000°C. At high temperature strength and creep resistance are still missing so further alloy advancement is expected to enhance these properties.

1.1.1 Tribology science

Tribology is basically the science and modernization of interrelating surfaces in relative movement. Tribology incorporates boundary layer interactions both among of solids and among of solids and fluids and/or gasses. Tribology means to advance wear, erosion and friction for a specific application case. Apart from this applications, tribology suggests high effectiveness and adequate reliability at the lowest potential assembling, manufacturing, and maintenance costs.

Wear be show one of the best usually experienced industrial issues, prompting normal substitution of parts. Particularly wear and abrasion resistance is not an inherent property of the material but also rely upon the tribological behaviour, for example, properties of materials tested, erodent grit size, test condition (temperature and pressure), atmosphere and equipment.

1.1.2 Wear

Wear of metals is likely the most vital yet at least known parts of tribology. It is positively the new of the three of points, friction, wear and lubrication, to pull in investigative consideration, despite the fact that its functional essentialness has been perceives throughout the ages.

Wear is not only a usual material property but it is also depends on the features of the engineering system which depend on velocity, temperature, load, hardness, region of outside material and the natural condition. Generally the fluctuation of material in wearing condition is the major cause of wear. It may be a direct result of surface removal or loss of material from one or both of two solid surfaces in relative motion. Generally wear happens through surface contacts [2]. But in case of erosion fluid flows over the surface results in disintegration and removal of materials from the contact surface takes place. Such as rock eroded by wind.

1.2 HISTORY OF Al

Aluminium was initially utilized in the industries regarding copper to frame aluminium bronzes, and this type of utilization provoked examiners to create methods of manufacturing, which is able for generating it at an expense which would warrant its utilization in huge amounts. It is definitely seen today that aluminium happens in nature just as oxides and that it is one of the stables oxides to be found, so stable that the principle technique for reducing it to its metallic state is by electrolysis method. In the beginning aluminium was used for reducing other oxides. It had the ability as a reducer, deoxidizer, or degasifier that it early turned into the companion of the steel and iron producer. It was the major cause, aluminium shortly turned into a genuine challenger of silicon, in spite of the high expense of aluminium in its initial days. Numerous were the amazing nature ascribed to this new metal. Many of these, on the other hand, existed just in the imagination of their promoters and were soon deny. Among the complete properties of aluminium, the following are may be the most vital [3]

a. when aluminium added to liquid iron, it will reduce iron oxide to metallic iron. Moreover, it will reduce CO or CO₂ gasses to free carbon and consequently degasify, calm the bath, and avoid blow holes during cooling and solidification. If the iron is adequately fluid, the Al₂O₃ formed will go to the surface; on the off chance that it is not, the Al₂O₃ will get to be snared in the iron, build the viscosity, and reason the iron to be more or less unsound.

b. When aluminium added in adequate quantities, 2 to 5 percent, aluminium will cause carbon to be totally precipitated as graphite and thus convert, for example, white cast iron into grey iron. If 10 to 20 percent aluminium is included, however, the carbon may all be in the combined form FeC.

c. The heat absorbed by the reduction of iron oxides is much lower than that the heat liberated by the oxidation of aluminium, it is clearly demonstrate by the use of thermite in welding iron, when aluminium is added to oxidized iron and steel, temperature will increase. When a small percentage of aluminium is added to the bath, fluidity will increase .it is mainly due to described fact, and not any considerable lowering of the melting point.

1.3 IMPORTANCE OF ALUMINIUM IN IRON AND STEEL

Aluminium is a valuable addition to a number of ferrous alloys and the resulting materials are of major industrial importance. The unique corrosion resistance, electrical and magnetic properties of alloy based Iron – Aluminium system have long stimulated the interest of metallurgists. In past decade aluminium was used as de-oxidiser in iron and steel. The addition of aluminium to iron in small proportions improves the deep drawing, hardenability, creep properties, damping capacity, notch sensitivity etc. An important advance in the metallurgy of high alloy steel occurred at 1930, when it was discovered that the addition of up to 10% aluminium to the iron- chromium and the iron – chromium- nickel alloys used in high temperature applications, increase the scale resistance considerably, in some case several fold.

1.4 MECHANICAL PROPERTY OF IRON-ALUMINUM ALLOY

Recently iron aluminides have been come into substantial interest as a prospective structural material for elevated temperature applications. But lack of ductility at ambient temperature and a decrease in strength above 600⁰ C have been measured which indicate their inability as better structural materials.

Intermetallic iron-aluminium alloys in comparison to conventional steel have a high measurable strength, low density, stiffness and wear resistance as well as excellent oxidation and corrosion properties, even at higher temperatures [4-5]. Furthermore, the raw materials and manufacturing costs of iron-aluminium alloys are low, especially in comparison to g-TiAl-alloys which have comparable material properties. Due to the excellent material characteristics, intermetallic iron-aluminium alloys qualify for many industrial applications, e.g. exhaust gas equipment, petrochemical installations as well as combustion engines and actuations [6–7]. However, the realization of such applications is limited due to the low machinability of intermetallic alloys which leads to high manufacturing costs of the parts.

Yensen and Gatward pioneered the earliest attempts at vacuum melting of Fe-Al alloy [8]. They prepare alloy up to 9% Al which possess measurable ductility but the yield and tensile strength of the alloys above 5 wt% Al were abnormally low indicating the presence of some in brittling factor such as oxygen contamination etc.

Hadfield, Styffe and Guillet have been studied the mechanical properties of iron-aluminium alloys. Who all conclude that that aluminium up to 5 percent has very little effect the mechanical properties of iron –aluminium alloy? While add aluminium greater than 5 percent, the iron -aluminium alloys are significantly increase in tension but it shows brittleness. Hadfield, whose specimens contained around 0.2 percent carbon, discovered the point of confinement of forgeability somewhere around 5.6 and 9.14 percent aluminium substance,

while Guillet discovered the utmost somewhere around 7.18 and 9.25 percent for alloys containing 0.8 percent carbon. The outcomes by these three specialists are demonstrated graphically in figure 1.1

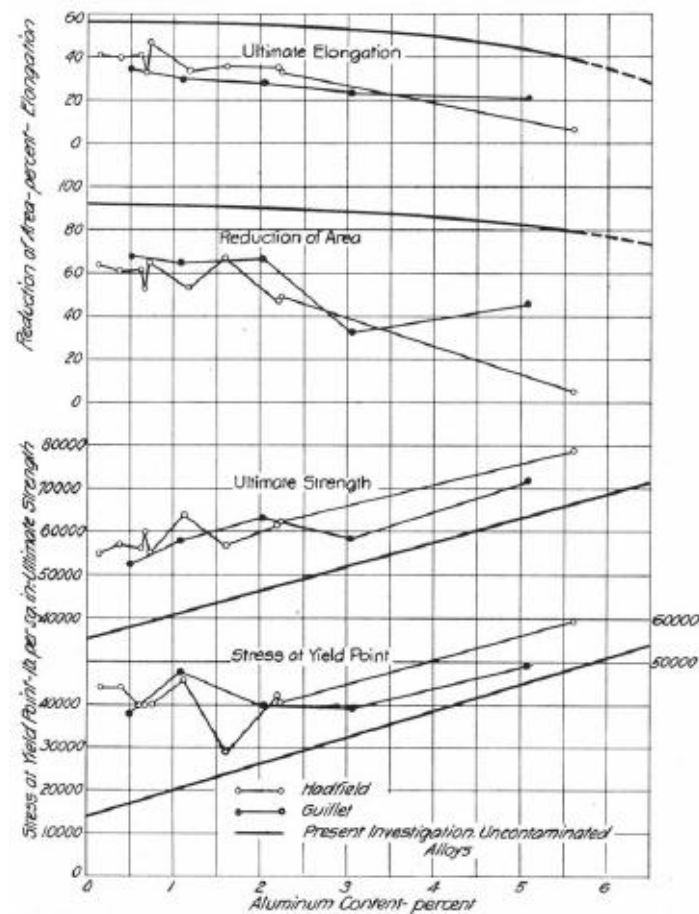


Fig 1.1- Mechanical properties of Iron –Aluminium alloy (T.D Yensen &W.A Gatward)

Sykes and Bampfylde were among the first, who spread attention to the diverse property of Fe-Al alloy. They studied on the mechanical, thermal, electrical properties melted in air Fe-Al alloys, particular interest in their investigation was the excellent oxidation resistance of alloys containing higher percentage of aluminium [9]. The existence of an ordered structure above 10

wt% was confirmed by both electrical and thermal measurements. They also emphasized the sensitivity of Fe-Al alloys to cracking under high thermal expansivity. It had also reported that the ductility decreases sharply with increase in aluminium concentration.

In another study by W. Justusson et al [10] the properties such as yield strength, tensile strength, elongation and reduction in area for binary Fe-Al alloys. The ratio of yield to tensile strength in this condition is essentially constant i.e. about 0.75% for alloys containing up to approximately 14%. Above this aluminium content the data are somewhat scattered, however a rapid fall in both yield and tensile strength is observed for the alloy containing 15 to 16% aluminium.

The decrease in ductility with increase in aluminium content up to 10% is similar for both water quenched condition. At higher aluminium contents the furnace cooled condition alloys show a slightly more rapid decrease in ductility with increasing aluminium. The small but definite decrease in ductility might be ascribed to the presence of order in the slowly cooled specimens since super lattice formation begins at the same aluminium level at which the decrease in ductility is being noted. However the sharp decrease in ductility, in either heat treated condition between 8 and 10% aluminium would appear to be from cause other than super lattice formation.

The foregoing data strongly indicate that maximum ductility of Iron-Aluminium alloys containing more than 10% aluminium is obtained by quenching from above the order disorder transformation temperature. However, the high susceptibility of Iron –Aluminium alloys to micro cracking induced by thermal stresses against for severe quench. The effect of

both quenching media and quenching temperature were studied to determine the conditions for retention of ductility in a 14% aluminium alloy.

The sharp drop in ductility observed in alloys containing more than 10% Aluminium might be explained on the basis other than the presence of interstitial elements. The hardness and tensile strength generally increases and the ductility decreases of most ordered systems.

Iron-Aluminium alloys like many other bcc materials which contain oxygen, carbon and nitrogen are susceptible to brittle fracture. This susceptibility is increased sharply by large grain size. For this reason vacuum melting, casting grain refinement and fabrication techniques were developed so as to achieve a minimum grain size in the finale wrought alloys.

1.5 MISCELLANEOUS USES OF ALUMINUM IN IRON AND STEEL

1.5.1 Heat resisting alloys

Aluminium greatly improves the heat resistance of iron. The increase in heat resistance is apparently due to the reduction by aluminium of any iron oxide formed at high temperature, a process that will continue as long as the rate of diffusion of aluminium exceeds the rate of oxidation of the iron. The optimum amount of aluminium necessary to produce satisfactory scale resistance in relatively pure iron depends up on the temperature at which the material is heated, on an average it should be at least 8% for temperatures of 900-1100⁰C and 10-13% for higher temperature. Much work has been done on the heat resistance of Iron-chromium alloys. Both chromium and aluminium increases scale resistance, but aluminium has by far greater effect.

1.5.2 Nitriding steels

The beneficial effect of aluminium steels stems from the nature and behaviour of aluminium nitrides. While a number other elements such as molybdenum, chromium, vanadium, titanium, tungsten form nitrides, aluminium nitride is more stable than the rest, with the possible exception of titanium nitride. In the absence of aluminium, the nitride case is frequently brittle

and spalls readily. Aluminium also inhibits the formation of braunite (a eutectoid of iron and nitrogen), the presence of which have an embrittling effect on the nitride case and cause spalling.

1.5.3 Aluminizing:

Aluminizing of iron base alloys become popular, by means of improving the corrosion resistance of materials in high temperature and this is useful in numerous power associated applications [11]. If aluminium enrichment takes place on the surface of the piece, this ensure the development of an aluminium oxide scale on subsequent surface in high temperature oxidizing atmospheres, technically without affecting the mechanical properties of the piece. Aluminium oxide is exceptional as a protective oxide. It thickens very slowly due to its low intrinsic defect concentration and is chemically very stable. In addition, the relatively well developed methods of promoting keying of the oxide scale to the substrate are amenable to aluminium oxide forming materials, and this adequately takes care of problems associated with poor scale metal adherence.

1.5.4 Tool steel

An unusual application of aluminium as a means to conserve tungsten and other alloying elements was reported by Mitsche and onitsch [8]. The results of lathe tests reported by them indicate that the addition of 0.5% aluminium to Cr-Mo-V tool steels is equivalent to the addition of 1.3% tungsten. Recently work is being on progress at R.R.L., Bhubaneswar to develop alloys with higher concentration of aluminium and carbon to be used as promising high speed tool material.

In high alloy tool steels, such as the 18-4-1 grade, aluminium seemed to be ineffective, where as in low alloy steels it increased the resistance to softening at high operating temperature.

Mitsche and Onitsch explained this difference in behaviour by postulating that in the high alloy steels there is sufficient tungsten in the matrix to create “diffusion impeding” distortion of the lattice. In low alloy steels, the small quantity of tungsten present exists in the carbide and the aluminium, owing to its large atom size, then operates as a diffusion impeding element and thus performs a function similar to that of tungsten in high speed steels.

Chapter

2

LITERATURE REVIEW

2.1 Introduction

2.2 Phase diagram of Fe-Al alloy

2.3 Constitution of iron rich Fe-Al-C alloys

2.4 Factors affecting the ductility of Fe-Al alloy

2.4.1 Influence of annealing treatments in ductility

2.4.2 Influence of grain size on ductility

2.4.3 Influence of substitutional alloying on ductility

2.4.4 Influence of molybdenum on ductility

2.4.4 Influence of molybdenum on ductility

2.4.5 Influence of carbon on ductility

2.4.6 Effect of temperature on yield strength

2.5. Melting and working of Iron-Aluminium alloys

2.1 INTRODUCTION

At the present time significant devotion is being given to the growth of inter metallic, basically for elevated temperature operational applications. Poor ductility is one of the major problem of those alloys although they possess sufficient strength [12]. The strength and ductility can be enhance by refine the microstructure that is to refine the grain size or by adding a scattering of second phase particles [13].

2.2 PHASE DIAGRAM OF Fe-Al ALLOY

The phase diagram of the Fe –Al system is shown in the figure below from 0 to 80 wt% Al, which shows a continuous series of solid solution with iron. In this field, order-disorder as well as magnetic to nonmagnetic transformations are known to exist, since no phase changes are involved in these transformations, the boundaries are shown in the diagram as dashed and dotted lines. The regions in the alpha field have been marked with subscripts, thus n and m indicate nonmagnetic and magnetic regions respectively.

The Fe-Al system has a close gamma loop formed by the lowering of the A4 and the raising of the A3 transformation temperatures. The gamma field extends to 1or 1.2% aluminium. The solid solubility of aluminium in gamma loop depends on the purity of the alloy, especially with respect to carbon oxygen and probably nitrogen. According to Kubaschewski [14], the solid solubility of aluminium in disordered Fe up to 45 wt% basically depends on temperature.

According to Sykes and Evans [15], the change from the disordered to ordered structure of type Fe_3Al can be prevail for composition less than 13.9% aluminium by quenching 600°C , but not with higher aluminium contents .

Two ordered compound D03-ordered Fe_3Al and B2 ordered Fe-Al. Fe_3Al is stable at compositions around 27 at% aluminium below 552°C and B2 ordered FeAl is stable at composition between 23 and 54 at% Al again depending on temperature [14]. Dotted lines

The diagram is a phase diagram for the Aluminum-Iron system. The y-axis represents Temperature in degrees Celsius, ranging from 0 to 1600. The top x-axis represents Aluminum in Weight Per Cent, ranging from 5 to 60. The bottom x-axis represents Aluminum in Atomic Per Cent, ranging from 0 to 80. Key features include:

- Liquidus Lines:** A solid line from 1400°C at 0% Al to 1232°C at 60% Al, and a dashed line labeled 'c' from 1400°C at 0% Al to 1103°C at 60% Al.
- Phase Regions:** Liquid, α + Liq., α (Disordered Non-Magnetic), α_n (Disordered Non-Magnetic), α_m (Disordered Magnetic), α_{2n} (Ordered FeAl Type Non-Magnetic), $\alpha + \epsilon$, ϵ , $\epsilon + \zeta$, ζ , $\zeta + \eta$, $\eta + \theta$, θ + Liq., θ + Al, and θ + FeAl₃.
- Invariant Points:** 1400°, 1232°, 1103°, 768° (Curie Temperature), and 910°.
- Alloys:** FeAl₃ (Type Ordered α'_{1m}), Fe₃Al (Type Ordered α_{1n}), Fe₂Al₉ (η), and FeAl₃ θ .
- Other Labels:** 2%, 2%, k, a, b, d, e, f, g, h.

Sykes and Bamfylde [16] studied the properties of solid solutions of iron –aluminium alloys and found that alloys containing from 0 to 5% aluminium are ductile and can be hot worked. Alloys hold 5 to 16% Al cultivate cold shortness therefore; it is believe strongly to be hot worked. Alloys hold more than 16% Al cannot be worked. Alloys beyond the alpha-solid

solution field (hold greater than 36% aluminium) are not useful practically in ferrous metallurgy.

Palm and Inden [17] were experimentally studied the ternary Fe-Al-C system phase equilibrium. It is proved that an adequate amount of carbon in Fe-Al alloys shows the precipitation of the perovskite-type k-phase Fe_3AlC_x . the K-phase is basically used for the strengthen of Iron-Aluminium alloys with aluminium contents up to about 50 at% ,which place over the composition range of BCC disordered Iron-Aluminium alloys[18]. DO₃-ordered Fe_3Al alloys [19-23] and B₂-ordered FeAl alloys. The K-phase precipitation would normalized the atmospheric embrittlement. The major reason of this atmospheric embrittlement is hydrogen embrittlement. An 8.9 at%C in Fe_3Al alloy, which contains Fe–Al precipitation in a Fe_3AlC_x matrix, was studied previously [21].

2.3 CONSTITUTION OF IRON RICH Fe-Al-C ALLOYS

Another task has been started to examine Fe_3Al based Fe–Al–C alloys with low carbon contents from 1 to 3 at. %. In Fig. 2.2 a piece of the isothermal area of the Fe–Al–C system at 800 °C [11] with a wide synthesis scope of two-phase equilibria of Fe (Al, C) solid solution (a) what's more, Fe_3AlC_x (k) is demonstrated. The syntheses of the quickly examined nine Fe–Al–C alloys are checked by filled circles in Fig.2.2. The three arrangements of alloys relate to three diverse tie-lines of the two-phase equilibrium $\alpha+k$ at 800 °C to look at the properties as a component of volume parts of phase with same composition for each tie-line.

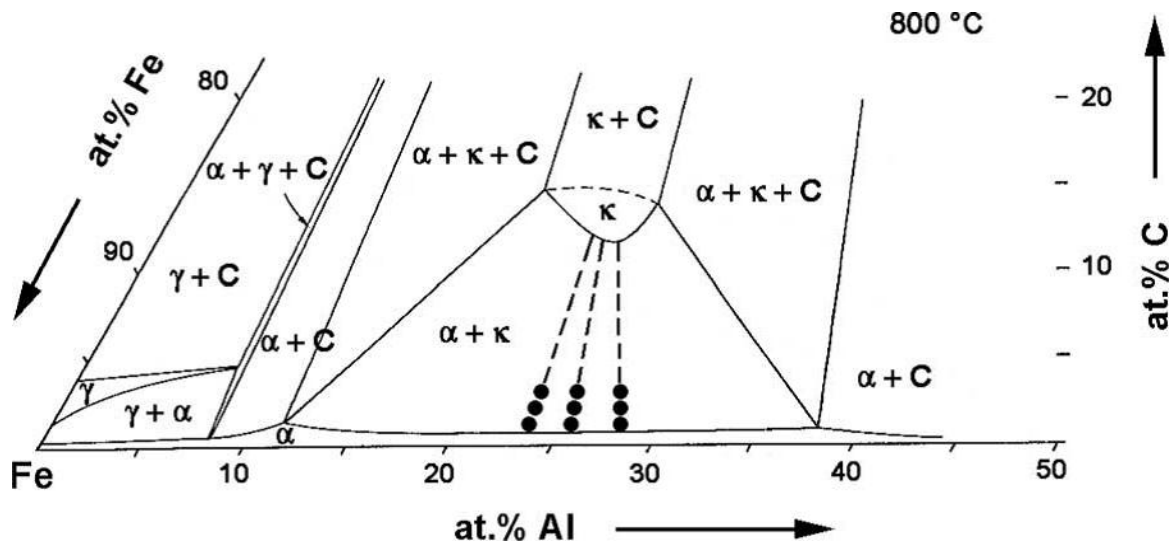


Fig.2.2 Fe-rich part of the, isothermal section of the ternary Fe–Al–C system at 800°C, according to [24].

The phase in these diagrams is designated as follows:

α : Solid solution of aluminium in alpha iron

γ : Solid solution of aluminium in gamma iron with varying carbon contents

C : Graphite

K : double carbide of iron and aluminium

The lattice parameters of alpha were found to range from 2.853 to 2.906 Å⁰, and those of gamma iron from 3.606 to 3.640 Å⁰. the exact composition of the double carbide k has not been determined with precision; however, it was found that the ratio of carbon to aluminium in the carbide was approximately 1 to 4.4. The double carbide was found to be ferromagnetic; it crystallizes as a face-centred cube with a lattice parameter of 3.719 to 3.780. From microscopic observation Morral [25] come to an end that the carbon fulfilled of K-phase is about 4% and the Al employ the corners of the elementary cube and Iron atoms occupy the centres of its face. It is hard and brittle ferromagnetic phase, its metal creation relating to Fe₃Al yet containing

additionally around 4% carbon. In spite of the fact that the arrangement of the atoms in the unit cell relates to a metal creation of Fe_3Al , this stage is not to be mistaken for the ordered structure of the kind Fe_3Al , which exists in the alpha field of the Iron-Aluminium alloy.

2.4 FACTORS AFFECTING THE DUCTILITY OF Fe-Al ALLOY

Significant effort has been dedicated throughout the most recent period to the progression of iron aluminides. It is most suitable materials for elevated temperature applications, where great oxidation and erosion resistance, consolidated with sensible quality, may be used. Some factor has restrict the advantage of these materials such as poor formability and ductility especially at room temperature. Different factors which influence the ductility of Iron-Aluminium alloy are as per the following:

2.4.1. Influence of annealing treatments in ductility:

It is currently settled that when iron aluminides was cooled from elevated temperature, vast quantity of voids formations takes place, Such voids are the major cause of extensive hardening of the materials [26, 27] apparently by voids going about as solute for pinning dislocations, while opportunity totals, for example, dislocation loops [28] and voids [29] might likewise bring about comparable hardening.

When alloys got Furnace cooling, which gives liberty to a genuinely high vacancy concentration, is provided genuinely low ductility for these combinations, when alloys got moderate cooling from very high temperature and a long annealing at low temperature prompts continuously enhanced ductility. Similar upgrades of ductility by vacancy evacuation have been obtained by various investigators [30, 31, 32].

Pang and Kumar [32] has been evaluated the relationship in the middle of embrittlement and hardening by vacancies in more details, as abridged in Fig.2.3, demonstrating the yield stretch after distinctive high temperature quenches, low temperature ageing, annealing, and the related tensile ductility. It should be noticed that these outcomes were acquired on a Fe±40Al alloy containing additionally 0.6%carbon, and this material contained some carbon as genuinely expansive rod like (Fe₃AlC) carbides, which might themselves assume some part in influencing fracture [32]. Among high temperature annealing and consequent ageing, some piece of the carbon may dissolve and precipitate [32] and hence annealing impacts reported may be compound impacts because of both vacancy and to carbon impacts. At the same time, the cooperation of lattice vacancies and interstitial C atoms is prone to adjust the mobility and inclination to agglomeration of vacancy defects [32]. The filled symbol data points of Fig. 3 demonstrate the impact of ageing at around 400° C, beginning from a high temperature extruded state, on yield stress and ductility: the impact of such ageing is a consistent diminishment of stress (from around 500 MPa to near300 MPa) and an attendant increment of ductility (from almost 2% to over 4%). The open symbol data points in Fig.2.3 demonstrate the outcomes of a few trials on quenched material which is therefore aged at distinctive temperatures, with mechanical testing did at several times at the same time of ageing. These information show, interestingly, that there is some slight age hardening, most likely connected with the carbon precipitation, and in the meantime a prominent embrittlement. One such age hardening-embrittlement cycle is shown by the arrangement of arrows in Fig.2.3. Resulting subsequent annealing to soften prompts an increment in ductility once more.

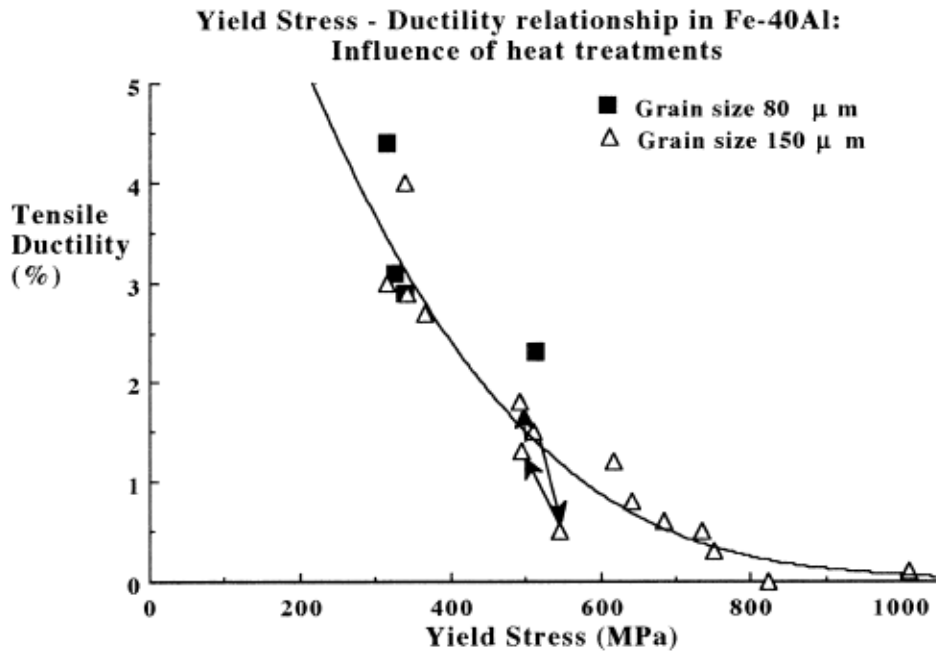


Fig2.3. Influence of heat treatments on yield stress and tensile ductility of Fe±40Al containing 0.6% carbon [32].

2.4.2 Influence of grain size on ductility

It is well proved that grain refinement is a wonderful path to improve ductility and it is also a effective to achieve about a brittle to ductile transition [33]. These results are concluded from the dependence of the yield stress on the grain size, for the beginning of plastic flow, as characterize by the Hall±Petch relationship ($\sigma_Y = \sigma_i + k_y$) and from the similar reliance of the fracture stress, characterised by a smaller (or zero) value of internal stress (σ_i) and a higher value of the grain size dependency slope k_f .

At the same time few scientists have announced an increment in ductility as the grain size is minimized different times it is accounted for that grain size refinement has just a minor impact on ductility.

2.4.3 Influence of substitutional alloying on ductility

Some investigator has been inspected the influence of substitutional alloying on ductility. They has been inspected in incredible subtle element for alloys containing around 28% Al [31±34], where DO3 order structure may be achieved, with less effort gave an account of the B2 combinations containing 40% Al or more [34]. Effects of this type of alloying on Fe-28Al-based alloys are outlined in Fig.2.4, where tensile ductility and yield stress are demonstrated. The current examination will consider changes of stress and ductility regarding this type of alloying, taking that every other parameter are constant, e.g. test environment grain size, strain rate, and so on.

In this test different alloying increments were utilized as shown in fig.2.4 and results in, for the binary alloys the grain size increased from around 50 to 100mm, or with Cr expansion, to almost 30 mm with extensive augmentations of Nb, MO or W. Such decreases of grain size don't prompt significant changes of ductility. When Cr is added to the binary Fe±28Al alloy, the ductility of this alloy increases. This sensational effect demonstrated in Fig. 5. This increment was initially credited to changes of plasticity of the material, yet has been connected with changes in the way of surface films and the degree of natural embrittlement [35, 36]. It is approved that natural embrittlement effect and some nature of the surface films created before or after testing is the major cause for all the progressions of ductility as shown in Fig. 2.4. It should be noted that all the alloys examined here show DO3 arrange after annealing at gentle temperatures, and the effects found may be considerably affected by slight changes in this order.

Influence of Alloying Additions on Strength and Ductility: Fe-28Al

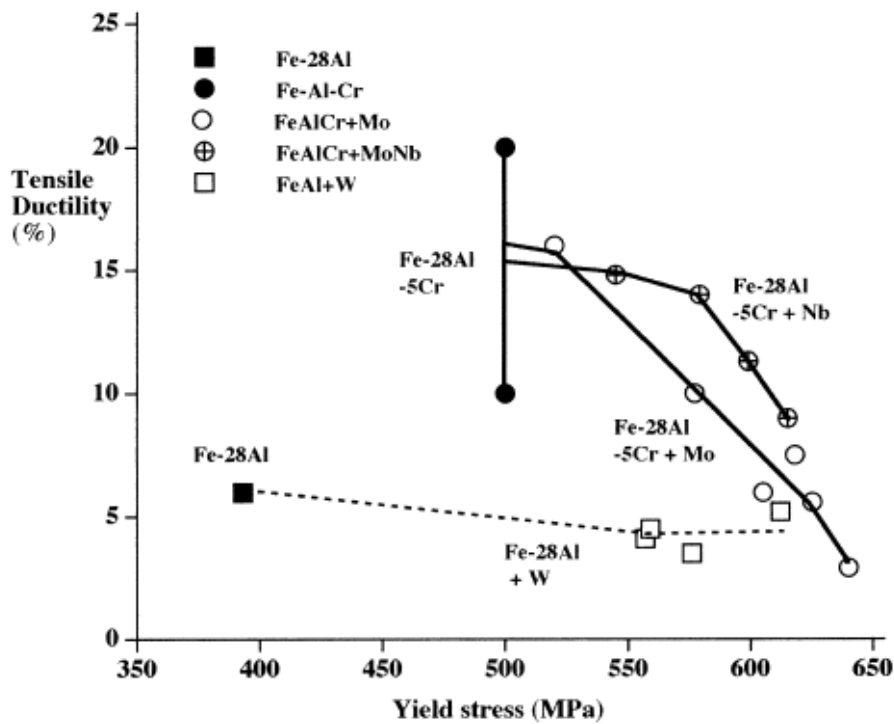


Fig -2.4 Changes of yield stress and tensile ductility with additions of various alloying elements (Mo, Nb, W)

Fig. 2.4 demonstrates that, with the alloying of any expansion of Nb, Mo or W prompts a dynamic loss of ductility. But alloying of Cr gives opposite result, it increases the ductility. Hardening and embrittlement happen when the alloying increases are dissolved as solute (e.g. $0.5 \pm 1\%$ Mo) or as second stage intermetallic or carbide particles (extensive increases of every last one of solutes analysed). Nevertheless, for the Fe \pm 28Al \pm 5Cr intermetallic base it is conceivable to attain strengthening (for instance to a yield stress close to 600MPa) by Mo and especially by Nb increases without sensational loss of ductility.

Although the ternary (or quaternary) augmentations to Fe \pm 28Al (+Cr) can strengthen and lead to just a steady loss of ductility, there is no proof that alloying with any substitutional component (counting Cr) to Fe \pm 45Al delivers any valuable impacts. In this study, even the addition of Cr prompts a fall in ductility and this for any testing environment. Some different studies have inspected alloying increases to FeAl alloys, for example [37], and have ordinarily

viewed as alloying addition that prompts second phase precipitation. Gaydosh et al. [37] considered increases of B and C alone to the Fe±40Al base, and in addition little augmentations of substitutional components, for example, Zr and Hf, furthermore joined increments of the light and the heavy components. The main material indicating enhanced room temperature ductility over the parallel base alloys was the one containing both Zr and B, with neither Zr alone, C alone, nor C+B alone enhancing ductility. The change of ductility saw for this situation may be because of the impact of B in increasing grain boundary strength, albeit there may likewise be an impact of particles of Zr intermetallic or borides on expanding ductility-by having a tendency to homogenize slip-or on diminishing ductility-if the coarse particles lead to stress concentrations and hence nucleate cracks.

2.4.4 Influence of molybdenum on ductility

The expansion of molybdenum result in a decrease in grain size for hot rolled and recrystallized specimens [37]. Tensile tests were directed on Fe-28Al-1 TiB₂ alloys of 0.5 and 2 at% MO. It was discovered that strength was not influenced by expansion of 0.5 and 1% MO. however expansion of 2 at% MO expanded the strength marginally at all temperatures and builds the ultimate strength of temperatures over 400°C. Ductility at all temperatures diminished with the expansion of more than .5% MO.

2.4.5 Influence of carbon on ductility

The impact of carbon on the mechanical properties of iron-Aluminium compounds is most fascinating one. At moderately low carbon substance, the transition temperature increments with expanding carbon. There is positive proof that for most extreme ductility, particularly in the 10 to 16 wt% Al; the ductility is higher with the bring down the carbon. In alloys with under 10 wt% Al and carbon substance up to a few wt%, 10 to 15 % ductility is held regardless of heat treatment.

2.4.6 Effect of temperature on yield strength

Near stoichiometric and iron rich Fe-Al alloy specimens by mechanical testing and post-testing examination have established the following. The yield strength of Iron-aluminium alloy is independent of temperature at low temperature but at higher temperature (above 500k for the near stoichiometric alloy and above 800k for the Iron rich alloy) decreases rapidly; At low temperature the yield strength decreases with increasing deviation from stoichiometry but at higher temperature increases with increasing deviation from stoichiometry. it was observed that around 700 K brittle to ductile transition takes place with decreasing grain size[38]. As temperature increases ductility also increases but 1000⁰K ductility is minimum, which is apparently due to grain boundary cavitation.

In summary, the yield strength of polycrystalline iron-rich Fe-Al slowly decreases or is independent of temperature up to about 800-900 K, above which it decreases rapidly and that the yield strength also increases with increasing aluminium content.

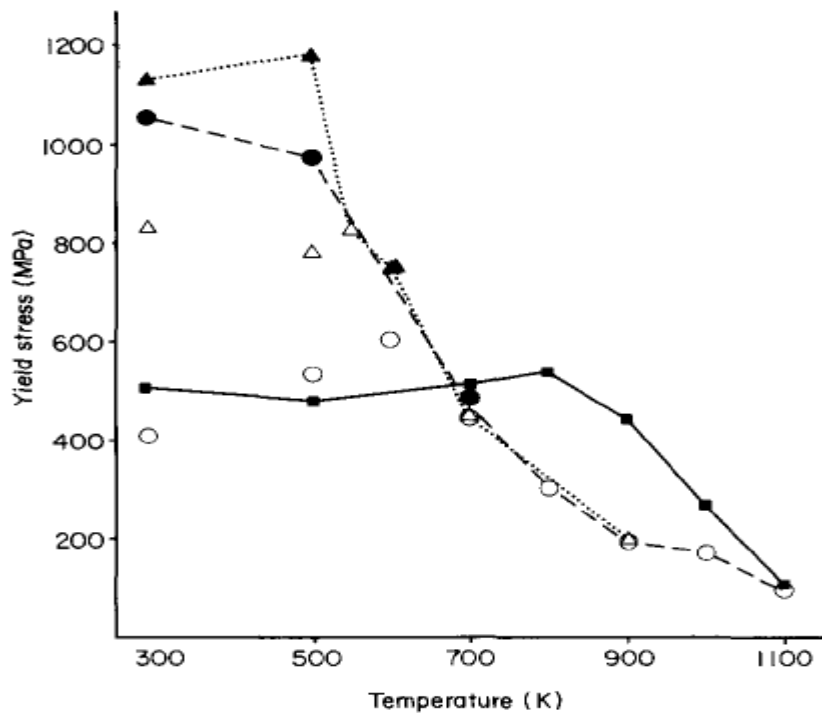


Fig-2.5 yield strength with respect to testing temperature for iron rich Iron-Aluminium alloy [39].

2.5. MELTING AND WORKING OF Iron-Aluminium ALLOYS

It is proposed that impressive trouble may be experienced in the assembling of Fe-Al alloys, unless uncommon methods are applied [4]. Sykes and Bamplydes suggest the accompanying induction furnace practice, where they claim brings about a satisfactory item. The iron is dissolved and after that deoxidized with silicon or titanium. Any slag present is skimmed off and after that aluminium is added. A basic lining is utilized. To decrease harm to the heater lining by oxide, expansion fluorspar to the charge are helpful.

Hot working of the binary alloys shows numerous problems. It is hard to work either hot or cold, the alloys containing high aluminium. Alloys with lower aluminium substance could be grouped into two groups containing 0-5% and 5-16% aluminium individually. Alloys in the first group can be hot worked without trouble; alloys in the second group are excessively brittle for cool and hot working. It has likewise been accounted for that, iron base alloys containing 4-8% aluminium and little amounts of titanium, if badly hot worked, were so coarse grained that 1 inch rounds would fracture when drop to the floor. Wire drawing practice for alloys in the first group is like that for high purity iron and shows little trouble. With higher aluminium substance in the alloys wire drawing is amazingly troublesome.

Chapter

3

EXPERIMENTAL PROCEDURE

3.1 Introduction

3.2 Material compositions

3.3 Metallographic

3.4 X-Ray diffraction studies

3.5 Heat treatment

3.6 Vickers hardness test

3.7 Air Jet Erosion Test Rig machine

3.1 INTRODUCTION

This section manages the points of interest of the experimental procedures followed in this study. This study comprise test specimen preparation, After samples preparation, the samples have been governed to a list of tests, e.g., metallographic of the surface ,X - ray diffraction analysis, heat treatment at different temperature(400⁰C,600⁰C,800⁰C and 1200⁰C), Vickers hardness test, air jet erosion test etc. The details of each procedure are described in this segment.

3.2 MATERIAL COMPOSITIONS

The chemical compositions of samples as shown in table below

Fe	Al	Si	Mn	C	W	Ni	Nb	Mo	Co
94.18	5.82	.12173	.16532	.10045	.45969	.1495	.0038	.09846	0.00635
Ti	Zn	Ce	B	Cu	Cr	V	S	P	
0.00190	0.00228	0.00591	0.00170	0.03303	0.0182	.0024	.027	.02655	

Table-3.1 chemical composition of samples

3.3 METALLOGRAPHY

In the beginning specimens were placed on a belt grinder for microstructure study. During grinding, specimens were moved front and back through the surface of the flat belt grinder. During grinding operation, samples were kept cool by dropping into water time to time. When belt grinding was done, samples were polished by a series of emery papers. It contains sequentially finer abrasive grains such as grades of 1/0, 2/0, 3/0 and at last 4/0. The samples

were moved in perpendicular direction to the current scratches during each polishing operation.

When polishing through the series of emery papers was done then samples were polished by using rotating wheel covered with special type of cloth. This cloth was charged with abrasive and water. Finally samples were polished by diamond polishing. After polishing samples were carefully cleaned with soap water, and subsequently dried using a drier. The sample was then etched with freshly prepared etchant (80ml ethanol, 20ml HNO₃ 1gm picric acid) for microscopic examinations.

3.4 X-RAY DIFFRACTION STUDIES

X-ray diffraction method was utilized to recognize the diverse (crystalline) phases show in the specimens. XRD analysis was done using Ni-filtered Cu-K α radiation in a Philips X-ray diffractometer. The characteristic d-spacing of all conceivable values are taken from JCPDS cards and were compared with d-values obtained from XRD patterns to recognize the various X-ray peaks obtained.



Fig3.1 –XRD machine

3.5 HEAT TREATMENT

Four samples of the investigated Fe-Al alloys were taken and were subjected to muffle furnace. For sensitization operation the Fe-Al alloys samples were subjected to different temperatures, 400°C, 600⁰ C, 800⁰C and 1200⁰C for 2 hour for soaking in same muffle furnace followed by water quenching.

3.6 VICKERS HARDNESS TEST

Hardness is a measurement of resistance of a material to indentation, deformation by means of abrasion, impact, drilling, scratching. It is measured by hardness tests such as Rockwell Brinell, Knoop, or Vickers. Since there is no classic hardness scale, each test give its results in its unique measure.

The heat treated specimens were polished by emery papers of distinctive grit size for hardness estimation. Vickers Hardness test was completed at room temperature to quantify the hardness of the Fe-Al alloy specimens. The load was applied by the diamond indenter for 10 seconds during testing of all the heat treated specimens.

Ten reading for every heat treated specimen were taken starting with one point then onto the next through the central line of the Fe-Al alloy and found the average value of to get final hardness results. A load of 5 kg was applied to the sample for 10 seconds. At that point the depth of indentation was noted by a system installed in the PC of arbitrary hardness numbers. Then these values were changed to as far as obliged hardness numbers (as Brinelle's or Vickers hardness numbers).

3.7 AIR JET EROSION TEST RIG MACHINE

In on-going examination, an erosion apparatus of the 'sand blast' type was utilized as indicated in Fig.3.2. It is capable for making very reproducible erosive circumstances over an extensive

variety of particles sizes, speeds, incidence angles and particles flow rate, so as to produce quantitative information on materials and to study the mechanisms of damage. The test was conducted as per (ASTM G76 standards).

In this research, an air jet erosion test rig (ASTM G76) is used to test the erosion of samples. The schematic view of the testing machine is shown in Fig.-3.2



Fig.-3.2 Arrangement of erosion test rig. (1) Sand hopper, (2) Conveyor belt system for abrasive particles, (3) Pressure transducer, (4) Particle-air mixing chamber, (5) Nozzle, (6) X- Y and h axis assembly, (7) Sample holder.

An Air jet erosion test rig apparatus was utilized to test erosive wear of target materials in the present examination. Irregularly shaped silica sand was utilized as abrasive particles. The sample were mounted into the test stage straight underneath the nozzle with utilizing 1 cm stand of distance (separation between tip of the nozzle to surface of the sample) furthermore Samples were eroded with silica sand at different impingement angles (i.e. 30°, 60°, and 90) In the present examination, room temperature erosion test facility is used. The setup is fit for making a uniform erosive circumstance for assessing erosion wear resistance of the processed Fe-Al samples. Dry silica sand is utilized as the erodent. The particles delivered at a constant rate are made to flow with compressed air providing by air compressor to impact the sample, which can be fixed at different angles with respect to the flow direction of erodent utilizing a swivel and a movable sample clip. The samples were cleaned by polishing and weighed to an accuracy of ± 0.1 mg accuracy utilizing a precision electronic balance the surface of material eroded in the test apparatus for 10 min and weighed again to focus the weight reduction. The methodology is repeated for all specimens. The erosion test rig consists of an air compressor, an air particle mixing, a particle feeder, and accelerating chamber. The erodent particles are fed at constant rate from storage to the conveyor belt-type feeder and then mixing chamber. The compressed dry air is combined with the erodent particles in the mixing chamber. After mixing, mixture accelerated by going through a tungsten carbide converging nozzle of 5 mm diameter. These accelerated particles hit the sample, which could be held at different angles with respect to the accelerated erodent particles by using a movable sample holder.

The erosion resistance of variety of materials including ceramics, metals, polymers, coatings and composites can evaluate with the help of air jet erosion tester conforming to ASTM G 76 specifications.

Sl.NO.	Description	Required Parameters
1.	Angle of inclination of specimen during W.r.t. the jet of abrasive particles.	30 ⁰ , 60 ⁰ , 90 ⁰
2.	Air pressure	Upto 4 bar
3.	Air velocity	Upto 109 m/s
4.	Particle feed rate	8.26 gm/min
5.	Sample size	Approx. 75mmx25mmx6mm preferable
7.	Erodent	Dry sand
8.	Stand of distance	1cm
9.	X, Y and Z arrangement and inclination	To be provided
10.	accumulation of erodent after testing in removable enclosure	To be provided
11.	Sound and dust proof enclosure	To be provided
12.	Nozzle	5 mm diameter to be provided
13.	Other features	Air drier and Air filter must be installed in the system

Table 3.2 Technical Specification for Air Jet Erosion Test rig as per ASTM G76

Chapter

4

RESULT AND DISCUSSION

4.1 Microstructure analysis

4.1.1 Microstructure before heat treatment

4.1.2 Microstructure analysis after heat treatment

4.2 SEM-EDS Analysis

4.3 XRD Phase composition analysis

4.3.1 XRD before heat treatment

4.3.2 XRD after heat treatment

4.4 Vickers hardness test

4.5 Air Jet Erosion test

4.1 MICROSTRUCTURE ANALYSIS

4.1.1 Microstructure before heat treatment

The optical microstructure of the investigated Fe-Al alloy is illustrated in figure 1(a). This figure shows a polygonal grain structure. The black dots shown in microstructure figure are graphite due to carbon present in Fe-Al alloy. Aluminium when added to liquid iron will reduce iron oxide to metallic iron. Furthermore, it will reduce CO or CO₂ gasses to free carbon and subsequently degasify, calm the bath, and avoid blowholes amid solidification and cooling [8]. In the grain boundary homogeneously distributed rod-like k-phase Fe₃AlC_x is present. The k-phase provides strengthening of Fe-Al alloys with Al contents up to about 50 at.% which covers the composition range of B.C.C disordered Fe-Al alloys, DO₃-ordered Fe₃Al alloys and B2-ordered Fe-Al alloys. K-phase is basically ferromagnetic ordered structure of Fe₃AlC_x. K-phase is not shown clearly in microstructure figure [1] before heat treatment because k-phase is very fine before heat treatment.

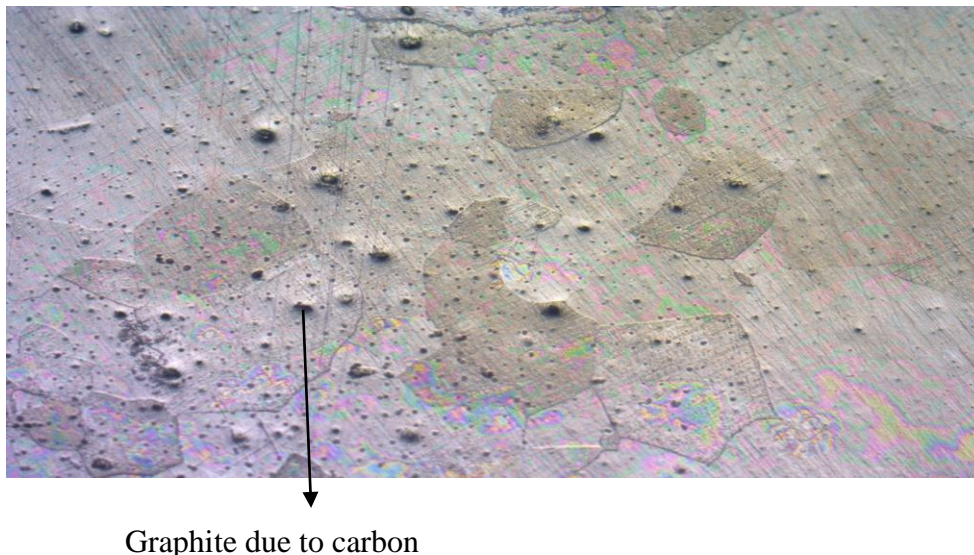


Fig 4.1: Microstructure of specimen before heat treatment



Fig.-(a) microstructure after heat treatment (400°C)

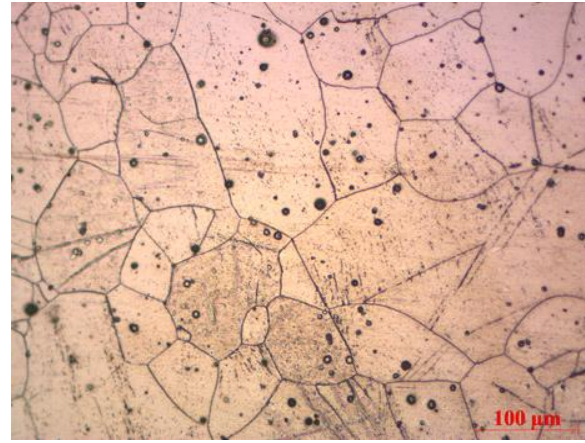


Fig-(b) microstructure after heat treatment (600°C)



Fig-(c) microstructure after heat treatment (800°C)

Rod like k-phase Fe_3AlC_x

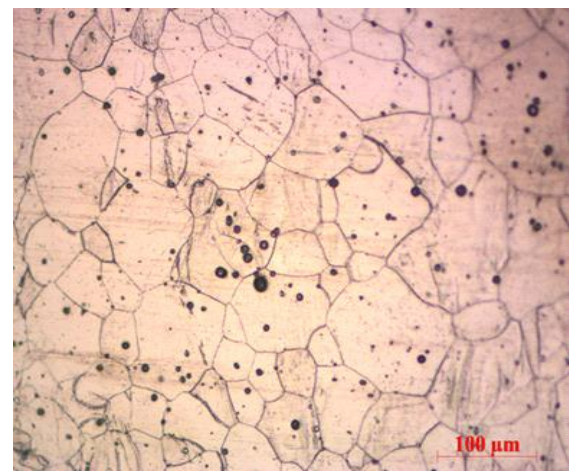


Fig- (d) microstructure after heat treatment (1200°C)

Fig-4.2 Microstructure of heat treated sample at temperature fig (a) 400° C (b) 600°C (c) 800°C and (d) 1200°C.

4.1.2 Microstructure analysis after heat treatment

The effect of heat treatment towards microstructure and phase transformation reveals from fig. 4.2. The microstructure of samples after heat treatment are significantly coarsened, due to coarsening of microstructure, rod like K-phase Fe_3AlC_x precipitates has also be coarsened. The size of K-phase Fe_3AlC_x precipitates has increased. Such fast coarsening kinetics of K-phase Fe_3AlC_x precipitates is due the high diffusivity of the interstitial carbon in the Fe_3Al

matrix and the fact that for the growth of the k-phase Fe_3AlC_x only the diffusion of carbon is needed. It can be stated that the performed heat treatment was detrimental to both—the room-temperature ductility and the high-temperature strength of all investigated alloys due to the observed coarsening of microstructures. There is a dramatic change in the microstructure of quenched from 1200°C sample as shown in fig 4.2 (d), the amount of graphite (black dots in micro structure) is comparatively low. May be, the carbon has combined with the iron and aluminium, unless it is precipitated in such finely divided state that it is invisible under the magnification used.

4.2. SEM-EDS ANALYSIS

The SEM-EDS analysis of the Fe-Al alloy specimen at 2500x magnification reveals the chemical composition of the structure.

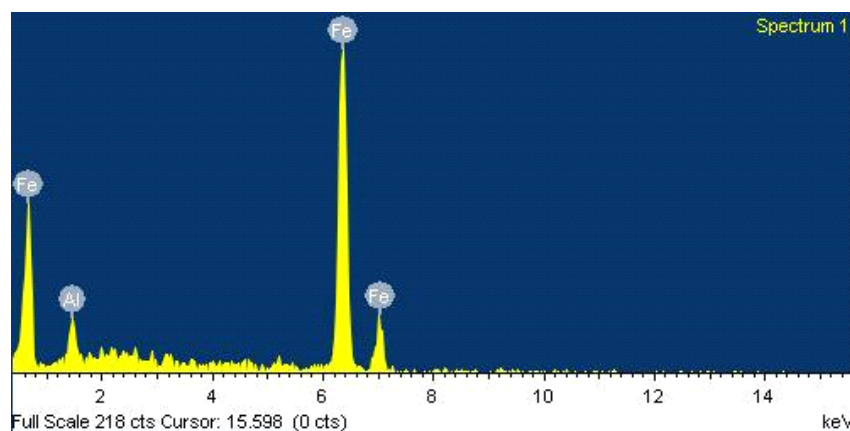


Fig 4.3 EDX analysis of Fe-Al alloy

Element	Weight%	Atomic%
Al K	5.82	11.34
Fe K	94.18	88.66
Totals	100.00	

Table4. 1: Chemical composition of the structure

Fig.4.32 and table 4.1 represent the EDS and the elemental analysis of Fe-Al alloy sample. It is concluded from EDS that the elemental composition obtained is very close to the parental Fe-Al alloy.

4.3 XRD PHASE COMPOSITION ANALYSIS

4.3.1 XRD before heat treatment

XRD plots between intensity and 2θ diffraction angle for different samples are shown in the graphs below. XRD was performed 30 KV and 20 mA using a Cu- $K\alpha$ target diffract meter. Scanning was done in angular range 2θ from 20° to 90° at a scanning speed of $5^\circ/\text{min}$. The profiles were analysed on computer by using X'Pert High Score Software to obtain the peak position and integrated intensities of Fe-Al alloy before heat treatment in (110), (200), and (211) planes. This indicates that it gives bcc structure. The observed sharp peak in the diffraction pattern, which justifies the highly ordered structure of alpha phase, can also be the cause for brittleness of Fe-Al alloy. It is noted that by XRD-analysis, only α ferrite phase is present, but k-phase is not present. It is mainly due to 0.1% C present in sample, which is too small to account for the amount of “extra” phase observed in XRD pattern.

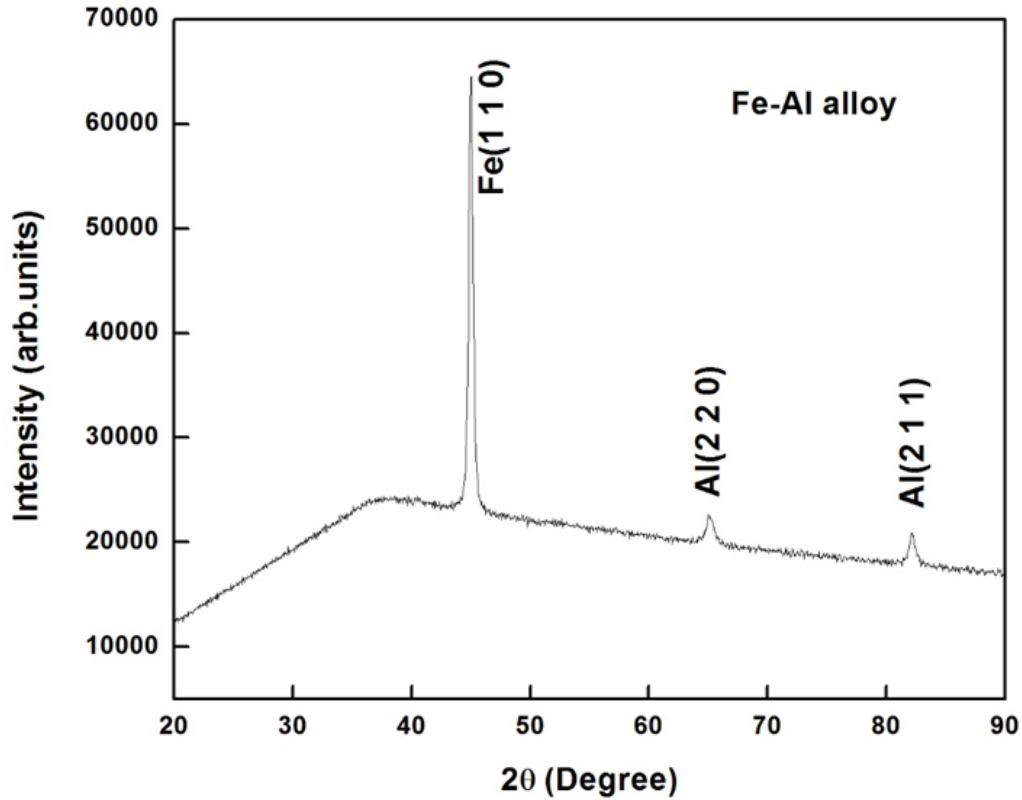


Fig 4.4- XRD pattern before heat treatment.

4.3.2 XRD after heat treatment

The effect of heat treatment towards phase transformations reveals from fig. 4.5 (a),(b),(c) and (d). The peak position and integrated intensities of Fe-Al alloy after heat treatment in different planes. Which indicates that it gives bcc structure for all heat treated sample. It is assumed that the area under the integrated intensity of each peak to be proportional to the quantity of material present. The XRD pattern of heat treated sample shows the presence of different phase such as Fe, Al and a new phase Al_5W . It is important to note that, XRD pattern of quenching from $1200^{\circ}C$ sample reveals a new phase Al_5W with higher intensity. This new phase provides hardness to specimen. It is also proved by doing Vickers hardness test of this specimen.

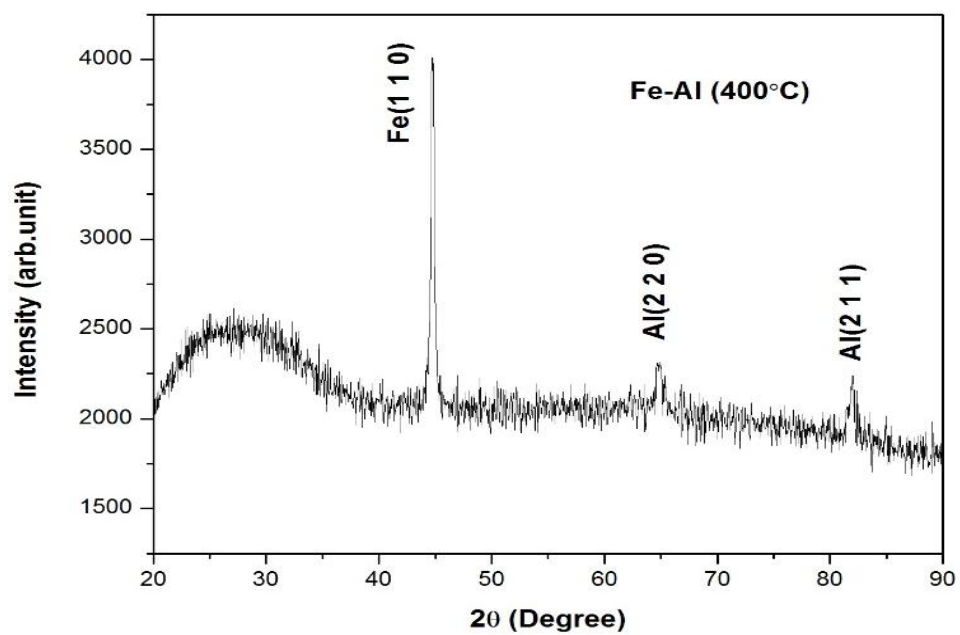


Fig – (a) XRD pattern of heat treated specimen (at 400°C)

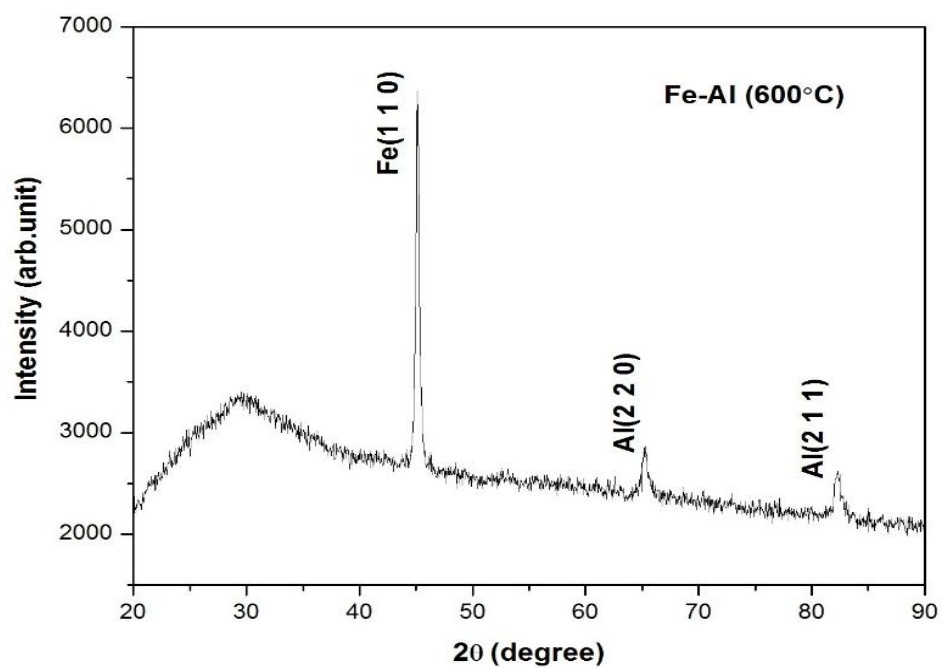


Fig – (b) XRD pattern of heat treated specimen (at 600°C)

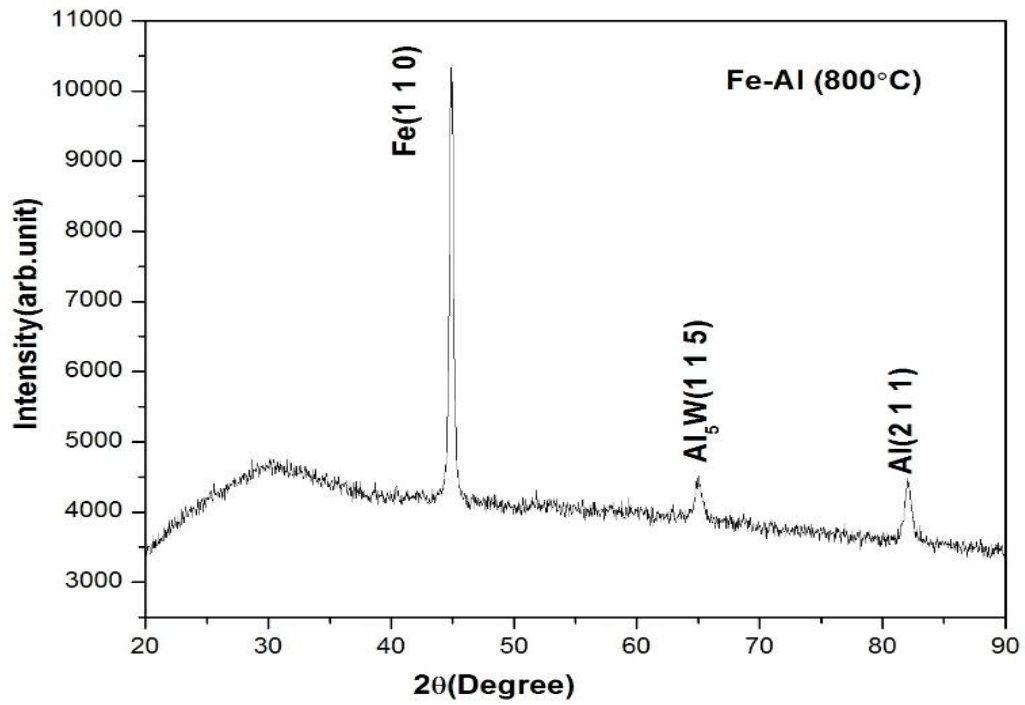


Fig – (c) XRD pattern of heat treated specimen (800°C)

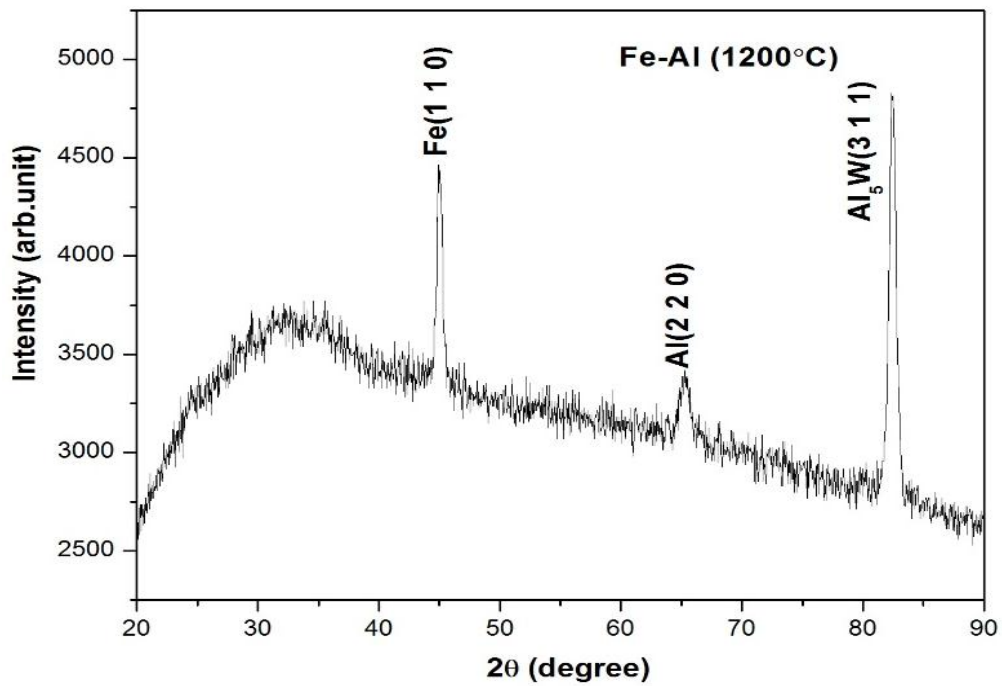


Fig – (d) XRD pattern of heat treated specimen (1200°C)

Fig 4.5 XRD pattern of heat treated specimen at temperature, fig (a) 400°C (b) 600°C (c) 800°C (d) 1200°C

4.4 VICKERS HARDNESS TEST

The hardness of the heat treated specimens (at 400°C, 600°C, 800°C and 1200°C) was measured in a Vickers Hardness testing machine with applying load of 5 N and a dwell time of 10 sec. Each hardness data is calculated from the average of 10 observations and are shown in the fig. 4.6 below. It is cleared from the graph that hardness decreases with heat treatment temperature from 400°C to 800°C, as shown in figure this decrement in hardness is very low. But in case of quenched from 1200°C specimen, it shows significantly increase in hardness as compare to other heat treated sample, it may be due to coarsening of k-phase and grain boundary as shown in microstructure of heat treated samples. It is concluded by XRD analysis of heat treated sample (1200°C), it shows a dramatically change in XRD pattern as compare to XRD pattern of other heat treated sample. XRD pattern of heat treated specimen (1200°C) shows a new phase Al_5W with higher intensity, basically this new phase with greater intensity is the major cause of hardness of heat treated (1200°C) specimen.

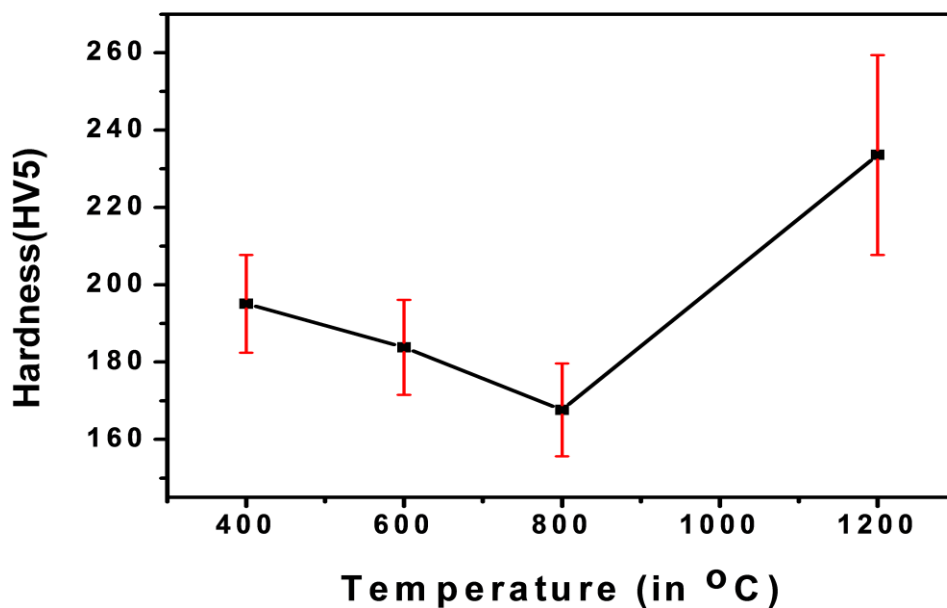


Fig-4.6 Hardness of specimens at different heat treatment temperature

4.5 AIR JET EROSION TEST

In air jet erosion test, solid abrasive particles i.e. dry silica sand hit or impinge on the surface of the material and cause material losses. The solid abrasive particles strike the surface at a certain speed and accordingly possess momentum and kinetic energy, which they convey to the surface during their impact and result in erosion wear. The particles are strike at distinctive angles from distinct stand of distance and at distinctive speeds to study the procedure parameters on the erosion wear rate. As the erodent particles strike the surface of the material, distinctive mechanisms of wear become an integral factor depending upon on the material attributes and the procedure parameters.

As we know that erosion rate depends on upon numerous variables size of impact particle, impact angles, stand of distance (it is separation between nozzle tips to surface of material), speed of impact particle, pressure, inner diameter of nozzle etc. In the present investigation, we considering the impact angles are the most influencing factor, so impact angles take as variable and all other are constant.

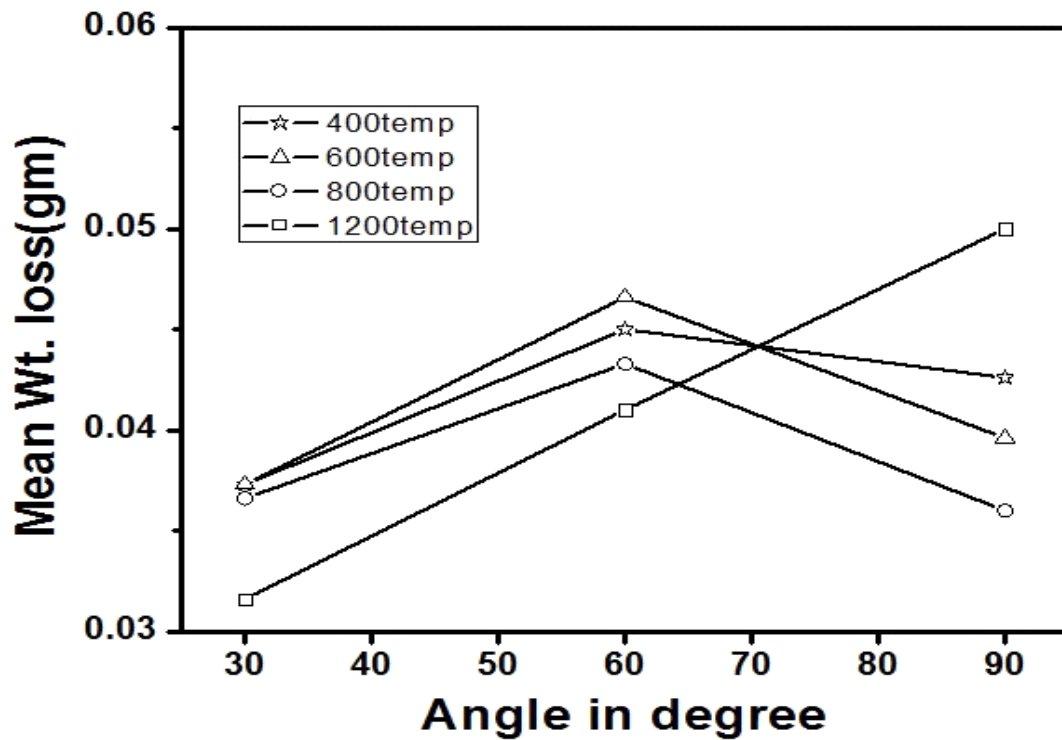


Fig – 4.7 Mean weight loss of heat treated sample at different temperature with respect to impact angles.

Fig. 4.7 shows the mean weight losses of heat treated at different temperature specimens at different impact angles.

It can be concluded from the graph that weight loss is maximum at 60° for all heat treated samples except water quenched from 1200°C sample. As the maximum weight loss occurs at 60° angles, it can be said that the erosion occurs by semi ductile mechanism. Rattan [40] has examined the impact of the angle of impingement of the solid particle on erosion rate and proposes that ductile materials show most extreme erosion at angle of impingement in the range of 15° to 30° and semi ductile materials shows greatest erosion at angle of impingement in the range of 45° to 60°, while brittle materials erosion is greatest at 90°. Water quenched from

1200°C sample shows maximum weight loss at 90°, as the maximum weight loss occurs at 90° angle, it can be said that the erosion occurs by brittle material.

Ibrahim [41] examined the connection of the impingement angle on the system of erosion wear and expressed that the normal and tangential components of speed of the erodent particles can be isolated and independently control the wear system.

At the point when particles strike, the specimen surface at a specific angle, the tangential components of abrasive particle speed results in plastic deformity of the composite [40]. Lower is the impingement angle, more prominent is the tangential component of the speed; therefore more prominent is the wear by plastic deformation. As in this specific composite erosion rate is higher at lower angles, accordingly erosion behaviour is ductile in nature [42].

Bayer [43] has recommended a relationship between the impact angle and the erosion rate in connection to ductile and brittle materials. As per Bayer ductile nature is predominant at lower angles of 20° to 30° while brittle nature of erosion is prevailing in higher angles (90°). Consequently the erosion is mostly because of micro machining and ploughing mechanism.

Chapter

5

CONCLUSIONS

5.1 Conclusions

CONCLUSIONS

The obtained results and their apposite discussion lead to the following conclusions:

- ❖ The microstructures of the investigated Fe-Al alloy shows a polygonal grain structure with homogeneously distributed plate-like k-phase Fe_3AlC_x precipitates. This provides strength of Fe-Al alloy. Phase is ferromagnetic ordered structure of Fe_3AlC .
- ❖ The microstructure of samples after heat treatment are significantly coarsened, due to coarsening of microstructure, rod like K-phase Fe_3AlC_x precipitates has also be coarsened. There is a dramatic change in the microstructure of quenched from 1200°C sample, the amount of graphite (black dots in micro structure) is comparatively low.
- ❖ The X-Ray diffraction analysis of the investigated Fe-Al alloy before and after heat treatment gives three peaks positions and integrated intensities in different plane. This indicates that it gives bcc structure. It is important to note that, XRD pattern of quenching from 1200°C sample reveals a new phase Al_5W with higher intensity. This new phase provides hardness to specimen. It is also proved by doing Vickers hardness test of this specimen.
- ❖ It is noted that by XRD-analysis before and after heat treatment, k-phase is not present. It is mainly due to 0.1% C present in sample, which is too small to account for the amount of “extra” phase observed in XRD pattern.
- ❖ Hardness decreases with heat treatment temperature from 400°C to 800°C . This decrement in hardness is very low. But in case of quenched from 1200°C specimen, it shows significantly increase in hardness as compare to other heat treated sample.
- ❖ It can be concluded by air jet erosion test that weight loss is maximum at 60° for all heat treated samples except water quenched from 1200°C sample. As the maximum weight loss occurs at 60° angles, it can be said that the erosion occurs by semi ductile mechanism. While water quenched from 1200°C sample shows maximum weight loss

at 90° , as the maximum weight loss occurs at 90° impact angle, it can be said that the erosion occurs by brittle material.

REFERENCES

REFERENCES

- [1] Palm, Martin. "Concepts derived from phase diagram studies for the strengthening of Fe–Al based alloys." *Intermetallics* 13.12 (2005): 1286-1295.
- [2] Ashby M. F. and Lim S. C. "Wear - mechanism maps." *Scripta Metallurgical et Materialia*. Volume 24, (1990): p. 805-810.
- [3] Yensen, Trygve Dewey, and Walter A. Gatward. "Magnetic and other properties of iron-aluminium alloys melted in vacuo." (1917).
- [4] Alman, D.E., Hawk, J.A., Tylczak, J.H., Dog̃an, C.P., Wilson, R.D., 2001, Wear of Iron-Aluminide Intermetallic-based Alloys and Composites by Hard Particles, *Wear*, 251/1–12: 875–884.
- [5] Stoloff, N.S., 1998, Iron Aluminides: Present Status and Future Prospects, *Materials Science and Engineering A*, 258/1–2: 1–14.
- [6] Deges, J., 2005, Eisenaluminide – Werkstoffe mit Zukunft, *DVS Berichte*, ;(235) 15–17.
- [7] Morris, D.G., Munoz-Morris, M.A., Chao, J., 2004, Development of High Strength, High Ductility and High Creep Resistant Iron Aluminide, *Intermetallics*, 12/7–9: 821–826.
- [8] Yensen, Trygve Dewey, and Walter A. Gatward. "Magnetic and other properties of iron-aluminium alloys melted in vacuo." (1917)
- [9] Sykes, C., and J. W. Bampfylde. "The physical properties of iron–aluminium alloys." *J Iron Steel Inst* 130 (1934): 389-410.

- [10] Justusson, W., V. F. Zackay, and E. R. Morgan. "The mechanical properties of iron-aluminum alloys." *Trans. ASM* 49 (1957): 905-923.
- [11] H.C Akuezue & D.P.Whittle,Metal science,vol. 17,January 1983,27.
- [12] D. G. Morris and M. A. Morris, Mechanical Properties of FeAl-ZrB₂ Alloys Prepared by Rapid Solidification, *Acta Metallurgica et Materialia*, Vol. 39,No. 8, 1991, pp. 1771-1779.
- [13] S.Strothers & K.Vedula,material science engg.78,1986,193
- [14] Kubaschewski O. Iron—binary phase diagrams. Berlin: Springer; 1982. p. 5.
- [15] Sykes .C & H.Evans, J. Iron steel Inst. Vol.131,1935,225-247
- [16] Sykes, C., and J. W. Bampfylde. "The physical properties of iron–aluminum alloys." *J Iron Steel Inst* 130 (1934): 389
- [17] Palm M, Inden G. *Intermetallics* 1995;3:443.
- [18] Baligidad RG, Radhakrishna A. *Mater Sci Eng* 2000; 281A:143.
- [19] Baligidad RG, Prakash U, Ramakrishna A, Rao PK, Ballal NB. *ISIJ Int* 1996;36:1453.
- [20] Baligidad RG, Radhakrishna A, Datta A, Rao VVR. *Mater Sci Eng* ,2001; 313A:117.
- [21] Sanders W, Sauthoff G. *Intermetallics* 1997;5:377.
- [22] Sharma G, Ramanujan TR, Kutty G, Tiwari GP. *Mater Sci Eng* 2000;278A:106.
- [23] Zhu SM, Guan XS, Shibata K, Iwasaki K. *Mater Trans* 2002;43:36.
- [24]Schneider, A., et al. "Microstructures and mechanical properties of Fe₃Al-based Fe–Al–C alloys." *Intermetallics* 13.12 (2005): 1322-1331.

- [25] Morral.F.R., Journal Iron and steel inst., Vol. 130, 1934, 419-428
- [26] Nagpal P, Baker I. Metall Trans 1990;21A:2281.[26]
- [27] Chang YA, Pike LM, Liu CT, Bilbrey AR, Stone DS. Intermetallics 1993;1:107.
- [28] Morris MA, George O, Morris DG. Mater Sci Eng, 1998;A258:99.
- [29] Morris DG, Joye JC, Leboeuf M. Phil Mag 1994;A69:961.
- [31] Gaydos DJ, Nathal MV. Scripta Metall Mater 1990;24:1281.
- [30] Gaydos DJ, Draper SL, Noebe RD, Nathal MV. Mater Sci Eng, 1992;A150:7.
- [32] Pang L, Kumar KS. Acta Mater 1998;46:4017.
- [33] Cottrell AH. The mechanical properties of matter. NY: J.H.Wiley, 1963.
- [34] Schneibel JH, George EP, Anderson IM. Intermetallics;1997;5:185.
- [35] McKamey CG, Liu CT. Scripta Metall Mater 1990;24:2119.
- [36] Balasubramaniam R. Scripta Mater 1996;34:127.
- [37] Gaydos DJ, Draper SL, Nathal MV. Metall Trans;1989;20A:1701.
- [38] Metallurgical transformation-A, Vol. 20A, April 1989, 751
- [39] Baker, I., and D. J. Gaydos. "Flow and fracture of Fe-Al." *Materials Science and Engineering* 96 (1987): 147-158.
- [40] R.Rattan, Jayashree Bijwe, "Influence of impingement angle on solid particle erosion of carbon fabric reinforced polyetherimide composite", Sci. Technol. Adv. Mater. 8, 023102,

2002

[41] A.T Ibrahim, A mechanisms for solid particle erosion in ductile and brittle materials, MS Thesis, Wichita State University, (1990).

[42] K.V.Pool,C.K.H.Dharan and I.Finnie,"Erosion Wear of Composite Materials", Sci.Technol. Adv. Mater. 9, 033002, 2008

[43] Bayer G. – Mechanical Wear Prediction and Prevention – Marcel Dekkar, Inc., New York: (1994) pp.396